Predation, evo-devo, and historical contingency: A nematode predator drives evolution of aggregative multicellularity

Kaitlin A. Schaal[1,2,*], Marco La Fortezza[2], & Gregory J. Velicer[2]

[1]Department of Evolution, Ecology & Behaviour, University of Liverpool, Liverpool, UK; [2]Institute of Integrative Biology, ETH Zürich, Zürich, Switzerland

* Corresponding author. Email: contact@kaitlinschaal.com

Abstract: Research into the evolution of multicellularity often focuses on clonal multicellularity, yet aggregative multicellularity (AM) may respond to different drivers and is also highly interesting evolutionarily, for example in its behavioral, regulatory, morphological, and social complexity and diversity. We investigate the potential for predation to shape AM evolution across different combinations of three species comprising a multi-trophic food web. Together in a three-species community, the fruiting bacterium *Myxococcus xanthus* is a mesopredator, while the bacterivorous nematode *Pristionchus pacificus* is apex predator and the bacterium *Escherichia coli* is a shared basal prey for both predators. The number and morphology of *M. xanthus* fruiting bodies is found to respond evolutionarily to nematodes, regardless of whether *E. coli* is present. *E. coli* alone with *M. xanthus* tends to reduce both fruiting body formation and spore production, but adding nematodes eliminates those negative effects. *M. xanthus* lineages with an ancestral antibiotic-resistance mutation evolved less overall, revealing strong historical contingency and suggesting potential tradeoffs between antibiotic-resistance and responsiveness to biotic selection. Our results suggest that predation both of and by mesopredators has played important roles in the evolution of aggregative multicellularity and reveal complex inter-trophic evolutionary interactions in a relatively simple three-species food web.

Introduction

The advent of clonal multicellularity (CM) is a Major Evolutionary Transition and is much studied (Stanley 1973; Bonner 1998; Ratcliff et al. 2012; Pentz et al. 2015; Herron 2016; Herron et al. 2022), but less attention has been given to understanding the origins, diversity, and evolutionary drivers of aggregative multicellularity (AM). Through AM, microbial cells that live independently for part of their life cycle come together to engage in and benefit from group behaviors. AM emerged multiple times, in both prokaryotes and eukaryotes, yet understanding of its evolutionary origins and what selective factors drive its diversification – potentially including predation on aggregative microbes – remains poor (La Fortezza and Velicer 2021; La Fortezza et al. 2022*b*, 2022*a*). Here we examine and compare multiple biotic selective pressures relevant to the evolution of AM, namely both predation of and predation by an aggregative microbe.

Many different types of organisms perform AM, suggesting that it has relevant adaptive benefits (La Fortezza et al. 2022*b*). The best-studied AM species are the amoeba *Dictyostelium discoideum* and the bacterium *Myxococcus xanthus,* the focus of this study. AM represents a way that organisms can overcome the biophysical limitations of single cells to increase their biological complexity. AM involves complex signaling repertoires that enable cells to encounter one another and regulate their coordinated behaviors, suggesting multi-step evolution and significant benefits to get there (La Fortezza et al. 2022*b*). It lacks the intrinsic control over relatedness that CM has, opening it up to threats from cheating (Grosberg and Strathmann 2007). That it persists further suggests adaptive benefits. Most known forms of AM involve two components: cells assembling into a macro-structure, and differentiation of some cells into a reproductive/stress-resistant sub-population. This suggests that AM may have originated as a mechanism for responding to biotic threats and/or to survive unfavorable environmental conditions (La Fortezza et al. 2022*b*). The latter hypothesis is supported by the formation of stress-resistant spores within aggregate structures in many AM systems in the lab, whereas the former hypothesis has been less investigated.

Predation has long been studied as a driving force in the evolutionary transition to multicellularity (Stanley 1973; Bonner 1998; Boraas et al. 1998; Claessen et al. 2014; Pentz et al. 2015; Kapsetaki et al. 2016; Herron et al. 2019), and indeed predation has been shown to select for clonal multicellularity (CM) in the lab (Herron et al. 2019). Although it has been hypothesized that AM might also provide protection from predation for a variety of aggregative microbes (Kessin et al. 1996; Velicer and Vos 2009; Dahl et al. 2011; Pérez et al. 2011; DePas et al. 2014; Müller et al. 2015), direct study of how predators of AM microbes influence the evolution of their aggregative behaviors and morphologies has been lacking.

We address this gap with a tri-trophic-level evolution experiment involving: (i) the social soil bacterium *M. xanthus* (order Myxococcales, aka

'myxobacteria' (Shimkets et al. 2006*a*; Velicer and Vos 2009)), which is a model organism for studying AM, (ii) *Pristionchus pacificus*, a nematode capable of preying on *M. xanthus* (this study), (iii) and *Escherichia coli,* a bacterium that serves as prey to both *P. pacificus* and *M. xanthus* (Hong and Sommer 2006; Morgan et al. 2010). *M. xanthus* aggregatively forms spore-filled fruiting bodies (FBs) upon starvation, as well as upon interacting with some other bacterial species (Kroos et al. 2025). *M. xanthus* is well known as a predator, swarming through soil in coordinated groups and preying on a wide range of other microbes, including gram-negative and gram-positive bacteria and fungi (Bull et al. 2002; Morgan et al. 2010; Mendes-Soares and Velicer 2013; Livingstone et al. 2017). *M. xanthus* presumably uses AM (FB formation) combined with sporulation to better survive low-nutrient conditions. However, it may also use FB formation to better survive predators in the environment. Selection from such predators may have thus contributed to the stunning diversification of fruiting-body morphologies observed among the myxobacteria (Shimkets et al. 2006*b*; Velicer and Vos 2009; La Fortezza et al. 2022*b*; Kroos et al. 2025), as well as among aggregative systems more broadly such as the dictyostelids (Bonner 2009).

Because *M. xanthus* and many other aggregative microbes (*e.g.*, the amoeba *D. discoideum*) are predators of other microbes as well as potential prey for higher-order predators, they are ideal for studying multi-step trophic webs in ecological and evolutionary experiments. *M. xanthus* predation on other bacteria has featured in multiple evolution experiments (MyxoEEs, see myxoee.org (Freund et al. 2024)). In MyxoEE-4, for example, *M. xanthus* adapted its foraging ability in response to prey abundance (Hillesland et al. 2009). In MyxoEE-6, it both adaptively evolved as a predator and drove evolution of prey responses in the lab, including changes in virulence traits (Nair et al. 2019; Nair and Velicer 2021). In MyxoEE-3, prey presence and identity were found to indirectly shape the evolution of *M. xanthus* fruiting body phenotypes (La Fortezza et al. 2022*a*).

Here we present the first evolution experiment in which *M. xanthus* functions as a mesopredator – both predator and prey – in a multi-level food web. This experiment was conducted to test effects of mesopredator nutrient-type (prey grown on nutrient-agar vs nutrient-agar only) and predation of the mesopredator on the evolution of *M. xanthus* features, including traits related to aggregative development.

Replicate populations of *M. xanthus* were allowed to evolve over 20 weekly growth cycles in each of four selective regimes that differed only in the presence or absence of two non-evolving biotic partners – *E. coli* as the basal prey and *P. pristionchus* as the apex predator. All are found in soils and may interact in their natural environment (Hong and Sommer 2006; Morgan et al. 2010). The experimental medium CFcc contains low levels of Casitone, sodium citrate, and sodium pyruvate (Mayrhofer et al. 2021). *M. xanthus* growth is limited through amino acid restriction, (Bretscher and Kaiser 1978), but *E. coli* growth is not (Kreth et al. 2013) (Figure 1A). Importantly, after depleting growth substrate from the nutrient agar, *M. xanthus* underwent aggregative development within each weekly evolution cycle in the absence of any biotic partners, creating the potential for addition of the basal prey and/or apex predator to impose direct selection on developmental features. After 20 cycles, we quantitatively compared several developmental traits – including fruiting body number, fruiting body density, and spore production – between evolved populations from each treatment and their ancestor, and between treatments. This allowed us to ask whether and how the basal prey and the apex predator, alone or in combination, altered the evolution of aggregative development by the mesopredator.

Moreover, observations during the evolution experiment led us to quantify how a single mutational difference between two genetic states of the *M. xanthus* ancestor, that determine sensitivity vs resistance to an antibiotic, altered evolutionary responses to the basal prey and apex predator. Single mutations have been observed to determine fitness trajectories in bacteria (Aggeli et al. 2021) Our findings contribute to the growing understanding of how very few genetic differences can profoundly influence how lineages respond evolutionarily to the same selective conditions in unexpected ways, and relatedly, how ultimate evolutionary outcomes can be contingent on small initial genetic differences (Blount et al. 2008, 2018). They also point to great complexity in interplay of forces shaping the evolution of AM mesopredator systems such as *D. dictyostelium* and *M. xanthus,* including not only who they meet as their predators and prey, but also evolutionary consequences of evolving resistance to antagonistic biotic compounds such as antibiotics.

Methods

Organisms

Our focal organism was *M. xanthus*, whose social traits and evolution in biotic context is of particular interest to us. Here we used the well-characterized *M. xanthus* lab strain GJV1 (Velicer et al. 2006) (strain 'S' in (Velicer et al. 1998)), as well as GJV2, a spontaneous mutant of GJV1 which is resistant to rifampicin (strain 'R' in (Velicer et al. 1998)). GJV2 differs from GJV1 by a single mutation in *rpoB*, the β-subunit of RNA polymerase (Zee et al. 2014). This mutation was expected to have little or no effect on fitness; we adopted this experimental design to allow us to directly compete evolved populations against the

reciprocally-marked ancestor during subsequent assays.

Our previous work indicates that *C. elegans* is not an effective predator of *M. xanthus* (Mayrhofer et al. 2021), so for this work we used *Pristionchus pacificus* PS312 (Hong and Sommer 2006) as the apex predator. We observed that under laboratory conditions, *P. pacificus* is able to grow and reproduce when *M. xanthus* is given as the only food source (Figure 2). For the basal prey, we used *E. coli* OP50, which is a commonly used laboratory prey of nematodes (Brenner 1974).

Bacterial growth conditions

We maintained 20%-glycerol freezer stocks of bacterial strains at -80 °C. We inoculated *M. xanthus* strains onto CTT 1.5% agar plates (Bretscher and Kaiser 1978) and incubated at 32 °C and 90% rH for 4 days, then transferred a portion of the colony into CTT liquid and incubated overnight at 32 °C with shaking at 300 rpm until the cultures reached mid-log phase (OD_{595} 0.2 - 0.8). We inoculated *E. coli* strains directly into lysogeny broth (LB) and incubated overnight at 32 °C with shaking at 300 rpm.

Culturing nematodes

We maintained freezer stocks of *P. pacificus* at -80 °C. We prepared freezer stocks according to Pires da Silva (Pires da Silva 2013). We collected worms from recently starved plates with Freezing Solution (100 µl/ml DMSO and 0.1 g/ml Dextran in water), aliquoted 1-ml volumes into freezer vials, and allowed them to freeze slowly in a Nalgene® Cryo 1°C Freezing Container containing isopropanol. To revive worms, we thawed an entire freezer vial, transferred the contents to a Falcon tube with a Pasteur pipette, added 10 ml of Thawing Solution (300 mg/L L-glutamine in M9 buffer [5 g/L NaCl, 6 g/L Na_2HPO_4, 3 g/L KH_2PO_4, and 1 mM $MgSO_4$ in water]), centrifuged for 1 min at 150 x *g*, and removed the supernatant. We then transferred the thawed worms to the edges of *E. coli* OP50 lawns on 2% agar NGM (Stiernagle 2006) or HGM (Kauffman et al. 2011) plates. We incubated the plates at 25 C and 50% rH.

Bleaching nematodes

We bleached *P. pacificus* as in Mayrhofer *et al.* (Mayrhofer et al. 2021) to create synchronized cultures to use in experiments. We washed nematodes from HGM plates using M9 buffer and collected them in a 15-ml Falcon tube. We centrifuged them for 1 min at 173 x *g* and removed all supernatant except 500 µl, to remove as much *E. coli* OP50 as possible. We added 1 ml of fresh M9 so that the total volume was 1.5 ml, then added 3 ml of bleaching solution (6 ml H_2O, 6 ml NaOCl 5%, 2 ml 5M NaOH) and bleached with periodic vortexing until most of the adult bodies had dissolved, up to 7 minutes. We removed the bleach from the released eggs by centrifuging for 1 min at 173 x *g*, removing all but 500 µl of supernatant, and adding 4.5 ml sterile water. We washed the eggs four times, and after the fourth wash removed all but 500 µl of supernatant and added 3.5 ml M9. We used a Pasteur pipette to transfer the egg suspension to a 6-cm petri dish and added 1 µg/ml gentamicin to prevent any possible *E. coli* contamination. We allowed the eggs to hatch overnight. To remove dauer pheromone and count the number of hatched J2 larvae, we centrifuged the worms in a 15-ml Falcon tube for 1 min at 173 x *g*, removed as much supernatant as possible, added M9 up to 1 ml, and counted in triplicate 1-µl aliquots plated on sterile CFcc 1.5% agar plates (Mayrhofer et al. 2021).

Nematode predation tests

To quantify population reduction of *M. xanthus* by *P. pacificus*, we prepared 6-cm petri dishes filled with 11 ml of CFcc 1.5% agar, inoculating ~2 x 10^6 CFUs GJV1 as the food source and spreading with glass beads. We added ~200 J2 *P. pacificus* larvae in 100 µl M9 or 100 µl of sterile M9 as a predator-free control and incubated at 25 °C and 50% rH. After 1 day, 4 days, and 7 days we destructively harvested all biological material from agar surfaces with a sterile scalpel and transferred to the center of a 9-cm CTT 0.5% agar plate. We measured the diameter of the swarm size of the surviving *M. xanthus* population after 4 days and used a standard curve relating swarm size to inoculum size to estimate *M. xanthus* population sizes (approach adapted from (Rendueles and Velicer 2017), Fig. S5). We calculated the area under the curve and used a general linear model to test for differences with and without worms.

To quantify reproduction of *P. pacificus* using only *M. xanthus* as a food source, we inoculated 3 x 10^9 cells of GJV1 or 300 µl sterile TPM buffer in the center of TPM 1.5% agar plates, picked 3 J4 *P. pacificus* larvae onto each plate, and incubated at 25 °C and 50% rH for 3 days. To count the worms, we washed the plates with 1 ml of TPM buffer, counted the number of worms present in 3 aliquots of 30 ul, and counted the number of worms remaining on each plate. For buffer plates, we only counted the worms present on the plates. We used a general linear model to compare the two treatments.

Evolution experiment

We isolated 6 clones each from GJV1 and GJV2 and named them 11-16 and 21-26, respectively (hereafter referred to collectively as 'A' for 'ancestor'). We used each of these clones to found four populations, one in each of the evolution treatments. The evolution treatments were *M. xanthus* evolving in monoculture (M), *M. xanthus* evolving in co-culture with non-evolving *E. coli* (ME), *M. xanthus* evolving in co-culture with non-evolving *P. pacificus* (MP), and *M. xanthus* evolving in co-culture with non-evolving *E. coli* and non-evolving *P. pacificus* (MEP). We performed the experiment on CFcc 1.5% agar plates (Hagen et al. 1978; Mayrhofer et al. 2021), which contain 0.015% casitone as the only source of amino acids. There are 17 amino acids which are essential for *M. xanthus* (Bretscher and Kaiser 1978), and the rich medium CTT on which it is often grown contains 1% casitone (Bretscher and Kaiser 1978). Therefore, monoculture growth of *M. xanthus* on experimental plates was limited by amino acid amounts. However, CFcc contains sodium pyruvate, which *E. coli* is able to grow on as a sole carbon source (Kreth et al. 2013), whereas *M. xanthus* is not. The presence of *E. coli* on CFcc medium in the ME and MEP treatments therefore increases nutrient availability to *M. xanthus* by converting inaccessible carbon sources into edible prey.

To initiate the experiment, we added ~2 x 10^6 CFUs of each founding clone, pre-mixed with ~10^9 CFUs of *E. coli* for ME and MEP treatments, to 6-cm petri dishes filled with 11 ml of CFcc 1.5% agar. We spread the bacterial inoculum with glass beads until dry, removed the glass beads, and added ~200 J2 *P. pacificus* larvae in 100 µl M9 (for MP and MEP treatments) or 100 µl of sterile M9 (for M and ME treatments). We sealed the plates with parafilm and incubated for 7 days at 25 °C and 50% rH.

To passage *M. xanthus* at the end of each cycle, we harvested the biological material from the surface of each evolution plate with a sterile scalpel and washed it into an Eppendorf tube with 1 ml of CFcc liquid with 1 µg/ml gentamicin to kill the *E. coli*. We incubated the tubes in a dry bath at 37 °C for 3 hrs (to kill the worms). We then transferred 1% of the volume of each culture to a new evolution plate (pre-mixed with either *E. coli* or buffer). We continued for a total of 20 cycles (Figure 1B). Six populations were lost due to contamination, leaving 42 evolved populations at the end of cycle 20.

At the end of even-numbered cycles, we transferred the remaining volume from the finished cycle to CTT liquid and allowed *M. xanthus* to grow up overnight in shaken culture at 32 °C and 300 rpm, then prepared 20%-glycerol freezer stocks.

Fruiting body morphology assay

We observed and quantified the fruiting body phenotypes of terminal evolved populations and their ancestors as in La Fortezza and Velicer (La Fortezza and Velicer 2021). We grew liquid cultures of cycle-20 evolved populations as described above. We diluted them and allowed them to shake overnight again in order to ensure that the resulting cultures would be as free from clumps as possible. We centrifuged them at 12,000 rpm for 5 min and resuspended to 5 x 10^9 CFUs/ml in TPM liquid. We poured 5 ml of CFcc 1.5% agar into 6-cm petri dishes and allowed to dry. We plated 10 µl of each population onto each of the two media types and allowed the spots to dry for 1 hr, then incubated at 25 ^{o}C and 50% rH for 7 days. Due to limitations on sample handling time during assay plate preparation, we processed in 5 blocks per replicate of 11 populations at a time. Each block also included GJV1 and GJV2 as internal controls. This resulted in 13 samples per block, and 20 total blocks.

After 7 days, we imaged the samples (Figure 1C) using an Olympus SZX16 microscope and Olympus DP80 camera together with cellSens software version 1.15 (Olympus, Tokyo, Japan), according to La Fortezza and Velicer (La Fortezza and Velicer 2021). Microscope, camera, and software settings were the same for all samples across all blocks and replicates. To check for correlations between fruiting body morphology and spore production, we then harvested all biological material using flame-sterilized scalpels, sonicated to disperse aggregates, and quantified spore production by counting the number of spores (identified by spherical shape and high refractivity) in a given area of a Neubauer improved hemocytometer.

Image processing

We analyzed the images using Fiji version 1.53q (Schindelin et al. 2012). We converted each image to 8-bit, removed dust particles and other non-bacterial parts of the image, and set the black-white threshold to capture all aggregates. We saved this information as an overlay which we applied to the original image to collect data on the aggregates. We measured morphological traits as in La Fortezza and Velicer (La Fortezza and Velicer 2021): number of aggregates, size of each aggregate (pixels^2), average grey value of each aggregate (density in La Fortezza and Velicer), standard deviation of grey values within each aggregate (density heterogeneity in La Fortezza and Velicer), and x and y coordinates of each aggregate.

Data analysis

We analyzed fruiting body morphological traits and spore production in R version 4.1.3 (R Core Team 2024) and RStudio version 2022.02.1+461 (RStudio Team 2020). We collected data on fruiting body morphology and spore production on two different media types, and we analyzed these data separately. We analyzed overall fruiting body morphology according to the method established by La Fortezza *et al*. (La Fortezza and Velicer 2021), by principal components analysis followed by PERMANOVA using the *adonis2* function in the *vegan* package (Oksanen et al. 2020) to check for effects of evolution environment. We further analyzed fruiting body traits individually using ANOVA to test for effects of evolution environment and of ancestral genotype (GJV1 or GJV2, from which we picked the 12 founding clones used to start the evolution experiment) followed by Dunnett tests for differences from the founding clones and Tukey HSD tests for differences among evolution treatments. We analyzed spore production data the same way, ANOVA for differences based on evolution environment and GJV1 versus GJV2 ancestry followed by Dunnett tests and Tukey HSD tests.

We tested morphological integration of fruiting body traits by analyzing eigenvector variance of the trait morphospace of the four developmental traits following previously established methods (Pavlicev et al. 2009; Machado et al. 2019; La Fortezza et al. 2022*a*). For this analysis, we included spore production as a trait. We calculated covariance matrices of the five traits for each evolution treatment individually and eigenvector variances (var(λ)) using *CalcEigenVar()* in the "evolqg" package (Melo et al. 2016).

Results

P. pacificus successfully preys on M. xanthus

To confirm whether *P. pacificus* acts as an apex predator in this system, we tested its ability to reproduce and consume *M. xanthus* as a sole food source. *P. pacificus* significantly reduces *M. xanthus* population size (Figure 2A; one-way ANOVA, $F_{1,20}$ = 6.94, p = 0.039), and is able to complete development to adulthood and reproduce successfully (Figure 2B; one-way ANOVA, $F_{1,20}$ = 32.73, p = 0.0001).

rpoB-mutant lineages show far less trait evolution in communities than wild-type lineages

We anticipated change in phenotypes related to multicellular development over evolutionary time in all treatments, as well as phenotypic diversification as a function of treatments, as such traits are relevant to nutrient levels, prey presence and type (La Fortezza et al. 2022*a*), and we hypothesized also to anti-predator defense (La Fortezza et al. 2022*b*). We therefore examined four traits related to fruiting body morphology in the evolved populations and their ancestral clones: the number of fruiting bodies produced by each population, their average size, their average density (darkness of color, with darker aggregates generally being more mature and containing more spores), and the average heterogeneity of density.

In the evolution experiment we included six lineages per treatment descending from GJV1 (wild-type) and six descending from GJV2 (spontaneous rifampicin-resistant *rpoB* mutant), to allow us to compete oppositely-marked strains head-to-head during follow-up assays. However, observations during the evolution experiment suggested that the GJV1 vs. GJV2 genotype difference may have influenced patterns of evolution. We therefore performed an initial analysis of the principal components of variation among the four traits based on ancestral genotype (GJV1 or GJV2), including the six ancestral clones of each and all surviving populations from the four evolution treatments from the final timepoint. We indeed found differences among these strains clones when grouped by ancestral genotype (Figure 3A; PERMANOVA for effect of ancestral genotype on morphology, $F_{4,48}$ = 4.13, p = 0.012); *rpoB*-mutant strains cluster more closely together, indicating that the evolved populations diverged less from the ancestral clones than did wild-type populations.

We then analyzed principal components of trait variation for wild-type and *rpoB* populations separately. Wild-type populations and their ancestral clones show significant variation among populations and from ancestral clones (Figure 3B; PERMANOVA for effect of treatment, $F_{4,21}$ = 16.99, p < 0.001). *rpoB*-mutant populations and their ancestral clones also vary (Figure 3D; PERMANOVA for effect of treatment, $F_{4,23}$ = 3.25, p < 0.001), although trait differences are smaller in magnitude than for wild-type lineages (Figure 4). Further, the two *rpoB* genotype groups show different patterns of evolved morphological integration, or pleiotropic correlation, across fruiting body traits (Figure S1).

The surprisingly lower degree of variation among GJV2-descended lineages indicates that the single *rpoB* mutation which separates GJV2 from GJV1 greatly inhibited diversification during the evolution experiment, resulting in evolved populations which

differ only slightly from their ancestors when undergoing development on the experimental medium. As GJV1- and GJV2-descended lineages showed unanticipated differences in levels of diversification, we analyzed individual trait change for the two groups separately.

The apex predator drives evolution of fruiting body number in antibiotic-sensitive strains

Two striking results emerged from the PCA of the fruiting body morphologies of GJV1 descendants. First, we see clear divergence of all three treatments with multi-species communities (ME, MP and MEP); Figure 3B, green, blue and purple ellipses, respectively) from the founding clones (A) and the M populations (Figure 3B red and yellow ellipses, respectively). Second, we also observe clear divergence of the two multi-species treatments that included nematodes (MP and MEP) from the one that did not (ME).

Quantifying individual traits (Figure 4), we see that MP and MEP populations produce more fruiting bodies that are also smaller, less dense, and less heterogenous, while the founding clones and the M populations produce fewer fruiting bodies that are relatively larger, denser, and more heterogenous (Figure 1C, representative images). In greater detail, populations which evolved in the presence of *P. pacificus* (MP and MEP) show significantly higher numbers of fruiting bodies than either the founding clones, M, or ME lineages (Figure 4; post-hoc Dunnett tests for differences from A and post-hoc Tukey HSD tests for differences among evolution environments, p's < 0.005). This effect is independent of the presence of *E. coli* (same Tukey HSD tests as above, $p_{MP:MEP}$ = 0.99). Fruiting body number of M and ME treatments did not diverge from the ancestral phenotype (Figure 4; same Dunnett tests as above, p's > 0.96). Intriguingly, GJV2 descendants do not show a similar trend of phenotypic change (Figure 4; one-way ANOVA for effect of treatment, $F_{4,23}$ = 0.76, p = 0.56). Together, this indicates that increasing the number of fruiting bodies produced by a population of a given size is an evolutionary response specific to the presence of worms, but that the *rpoB* mutation in the GJV2 lineages inhibits this response.

Evolution in multi-species communities reduces individual-fruiting-body trait values

The PCAs in Figure 3B and 3D suggest little overall divergence between phenotypes of populations that evolved in monoculture and phenotypes of the ancestral clones (*i.e.,* the red and yellow ellipses are largely overlapping, indicating that they represent groups with similar trait values). In line with this, the individual trait analyses (Figure 4) show that the M populations evolved to differ from the ancestral phenotype only in fruiting body size, and not at any of the other three traits. The average fruiting body size of the M populations increased significantly relative to their ancestor (post-hoc Dunnett tests for differences from A, p = 0.03) and was also greater than the average values for the other evolution treatments (post-hoc Tukey HSD tests for differences among evolution environments, $p_{M:ME}$ < 0.001, $p_{M:MP}$ = 0.003, $p_{M:MEP}$ = 0.019). In those other treatments, fruiting body size clearly (ME) or suggestively (MP, MEP) decreased relative to the ancestor (post-hoc Dunnett tests for differences from A, ME p < 0.002).

Contrary to the increase in fruiting body number seen in MP and MEP populations descending from GJV1, there are broad decreases in other trait values across all three treatments with multi-species communities (Figure 4). GJV1 descendants that evolved under ME, MP, or MEP conditions all form significantly less dense and less heterogeneous fruiting bodies than both the ancestor (post-hoc Dunnett tests for differences from A, p's < 0.001) and the M-evolved populations (post-hoc Tukey HSD tests for differences among evolution environments, p's < 0.005). That these traits did not also decrease among the M populations points to evolutionary responses specific to the presence of biotic partners rather than a generic response to abiotic conditions. Moreover, evolution in the presence of either prey or apex predator, or both, increased morphological trait integration (Figure S1). The ancestor has eigenvector variance of 0.5, showing partial correlation among the morphological traits (0 is no correlation, 1 is full trait correlation (Pavlicev et al. 2009)). This increases for M, and increases to nearly 1 for ME, MP, and MEP. Thus, evolution in multi-species communities drove greater integration of *M. xanthus* developmental traits than did evolution in single-species populations.

Populations descending from GJV2 also showed some evolution at traits other than fruiting body number, but changes were smaller overall than for GJV1-descendants (as expected from the PCA in Figure 3A). All evolution treatments except for ME form less-dense fruiting bodies than the ancestor (post-hoc Dunnett tests for differences from A, p's < 0.03). Only MEP populations show divergence in density heterogeneity, both from the ancestor (post-hoc Dunnett tests for differences from A, p = 0.049) and from M- and ME-evolved populations (post-hoc Tukey HSD tests for differences among evolution environments, p's < 0.02).

Interaction between the apex predator and basal prey causes unexpected phenotypic evolution

If the selective effects of the basal prey and the apex predator on *M. xanthus* phenotypic evolution were additive, we would expect trait values in the MEP treatment, which exposed *M. xanthus* to both, to fall in between those for ME and MP treatments. However, instead we see striking deviations from this expectation for two individual-fruiting body traits – density and density-heterogeneity (Fig. 4C-D). If one starts with MP as a reference point and then considers that the ME result would predict that the MEP value should be lower than the MP value under the assumption of linearity, we see that inclusion of E in the MEP populations has the opposite effect, causing these three trait values to evolve to higher levels than in the MP populations rather than lower. And using ME as the starting reference point, inclusion of P in the MEP treatment increases the trait values more than predicted from the ME and MP data alone. Thus, the effects of *E. coli* and *P. pacificus* on *M. xanthus* evolution interact in a nonlinear manner.

Nematodes prevent evolutionary reduction of M. xanthus sporulation caused by E. coli alone

Given the significant changes in fruiting body numbers and several traits of individual fruiting bodies, such as size, we hypothesized that there may be correlated changes in the number of spores produced by those populations and associated treatment-level effects. We paired each measure of fruiting body number and size with the number of spores counted from that plate (Figure S2). Spore production correlates positively with both of these traits (Table S1). For descendants of GJV1, the correlation with fruiting body size differs based on evolution environment (Table S1; two-way ANOVA for effects of size or area and treatment on spore production, $F_{4,16} = 3.132$, $p = 0.044$), but in every other case the effects are independent.

When looking at spore production only (Figure 5) overall across populations descended from both ancestors (GJV1 vs GJV2), most treatments showed no significant change or moderate increases in spore production. Exceptionally, however the ME populations decreased ~90% in spore production on average. The absence of a corresponding decrease in the MEP lines indicates that the presence of *P. pacificus* prevented selective effects of *E. coli* from evolutionarily degrading *M. xanthus* sporulation, perhaps simply due to the removal of *E. coli* by nematode predation.

Discussion

Here we characterize the phenotypic evolution of an aggregatively multicellular bacterium in a multi-trophic food web, with implications for understanding the evolution of biotic networks and aggregative developmental systems, including roles of historical contingency. The presence of a nematode predator of *M. xanthus* strongly impacts the evolution of both *M. xanthus* fruiting body morphology and spore production. *P. pacificus* had several evolutionary effects on *M. xanthus*, including (i) increased fruiting-body numbers after evolution in both the absence and presence of *E. coli* (Figure 4A; MP-vs-M and MEP-vs-ME), (ii) reduced fruiting body size, density, and density heterogeneity during evolution in the absence of *E. coli* (Figure 4B-D; MP-vs-M), (iii) mitigation of larger decreases in fruiting body density and density heterogeneity caused by evolution with *E. coli* alone (Figure 2C,D; MEP-vs-ME, and (iv) prevention of major decreases in spore production caused by evolution with *E. coli* alone (Figure 5A; MEP-vs-ME). Increased trait integration (Figure S1) suggests the presence of selection on development (Pavlicev and Hansen 2011).

Moreover, we found that just a single mutational difference between ancestral founding populations that confers antibiotic resistance profoundly impacted the evolvability of a mesopredator in response to both predator and prey of the mesopredator. Populations which descend from an ancestor carrying a single-base-pair mutation in *rpoB* underwent far less morphological change and diversification overall than populations lacking the mutation (Figures 3, 4, & S2). A previous study found differences between evolved populations descending from GJV1 and those descending from GJV2 in terms of colony-color evolution (Rendueles and Velicer 2017), showing additional evolutionary effects of GJV2's *rpoB* allele. The profound evolutionary consequences of this single mutation in our study may be due to the mutation causing systematic differences in what adaptive pathways are followed or to differences in the effects of similar adaptive pathways on the observed developmental phenotypes due to epistasis (Blount et al. 2018; Aggeli et al. 2021).

The evolutionary effects of an antibiotic-resistance mutation we observed raise intriguing questions for microbial mesopredators about possible evolutionary interactions between resisting higher-order predators, resisting antibiotic-mediated antagonisms from both conspecific and heterospecific microbes, and themselves preying on other microbes. It may be that resistance to antibiotics which target transcription may more generally come at a cost to an organism's ability to adapt to predators. Even such an aggressive (Vos and Velicer 2009; Rendueles et al. 2015; Rendueles and Velicer 2017) and probably well-defended microbe as *M. xanthus* (Findlay 2016; Mayrhofer et al.

2021) is likely to experience trade-offs as it deals with antagonism from competitors and predators. Future research could examine potential trade-offs between competition within a trophic level (*e.g.,* competition among strains or species) and selective pressure from higher trophic levels, as well as the role of antibiotics and resistance to them in these conflicts (Cornforth and Foster 2015).

We show that the basal prey and the apex predator in our experimental system in some cases had an interacting influence on trait changes in the mesopredator. Evolution in the presence of *E. coli* often led to the lowest values of morphological traits (Figures 3A-D & 4) and spore production (Figure 5) (La Fortezza et al. 2022*a*). In contrast, evolution in the presence of *P. pacificus* tended to lead to higher trait values, relative either to the ancestral phenotype and to the treatment with *E. coli* (Figure 4A) or just to the latter (Figure 4B-D). In the latter case, the presence of both organisms led to evolution of higher trait values than the presence of *P. pacificus* alone. This could indicate an effect like apparent competition between the two bacteria, where the basal prey boosts the apex predator's population, increasing the apex predator's effect on the mesopredator (Holt 1977; Holt et al. 1994; Holt and Bonsall 2017). Collectively, these patterns show clear evidence of evolution in response to an apex predator which affects developmental pathways in such a manner that phenotypic changes emerge across different environments, in both 2- and 3-level trophic communities.

Because *M. xanthus* undergoes development in the abiotic selective regime used in this experiment (CFcc agar), particular evolutionary changes in developmental traits may be adaptive *per se.* For example, populations that evolved in the presence of *P. pacificus* may produce more fruiting bodies because they evolved to form fruiting bodies faster in order to better survive predation. Loss of spore production by populations evolving with *E. coli* alone might reflect relaxed selection for sporulation because *E. coli* increases the level of resources available to *M. xanthus* by converting carbon sources inaccessible to *M. xanthus* alone into prey biomass. In this scenario, the phenotypic degradation we observed in the ME treatment could be due to generic adaptation to a high-resource environment (Velicer *et al.* 1998), rather than selection imposed by interactions with the prey itself. Testing among hypotheses to explain specific patterns of developmental-trait evolution across our treatments is of interest for future work.

P. pacificus drives the evolution of more fruiting bodies but not increased spore production (Figs. 4 and 5). In fact, spore production appears to respond as an independent trait to the presence of prey alone, as in La Fortezza and Velicer (La Fortezza and Velicer 2021), where spore production and fruiting body morphology evolved in an uncorrelated manner. This suggests that the aggregation step of multicellular development may have evolved separately from spore formation, possibly in response to predation pressures (La Fortezza et al. 2022*b*). This could be tested specifically by evolving a strain which is defective at fruiting body formation in pure culture (Velicer et al. 2000; Schaal et al. 2022) in the presence of the predator. It would also be interesting to see for how long the difference fruiting body numbers between the M and MP populations evolved here would be retained if both were to evolve further in conditions without the predator.

Brodie and Brodie (Brodie and Brodie 1999) proposed that adaptation in predator-prey relationships spanning multiple trophic-level steps be thought of as a process of escalation. That is, changes in the morphology or behavior of a mesopredator (even for traits not directly related to predation) would drive responsive adaptation in its prey, but adaptation of the mesopredator would be driven largely by its own predators and not by the prey. A previous study has shown that prey identity can strongly affect how *M. xanthus* fruiting body phenotypes evolve indirectly (La Fortezza et al. 2022*a*) but in that study the prey did not co-evolve with *M. xanthus,* as also in this study, and fruiting body formation was not under direct selection. A subsequent evolution experiment would be of interest to test whether prey-presence and prey-type effects on *mesopredator* AM evolution would be observed when an apex predator is present and when all parties can freely co-evolve, as well as to examine relative effects of the apex predator and basal prey.

How predation and multicellular development relate to each other in the historical evolution of the myxobacteria is not yet well understood. Future comprehensive identification and phylogenetic analysis of the genes involved in both behaviors will improve understanding of their relative origins. While many selective forces are likely shape the evolution and diversification of aggregative multicellular systems (Bonner 1998; La Fortezza et al. 2022*b*), our results point to not only predation by mesopredators, but also predation of them, playing important roles.

Acknowledgements

We thank Hinrich Schulenburg, Ralf Sommer, and Peter Zee for advice and discussion. Some strains were provided by the CGC, which is funded by NIH Office of Research Infrastructure Programs (P40 OD010440). This research was supported in part by an EMBO Long-Term Fellowship (ALTF 1208–2017) to M.L.F. and in part by Swiss National Science Foundation (SNSF) grants 31003A_16005 and 310030B_182830 to G.J.V.

Literature Cited

Aggeli, D., Y. Li, and G. Sherlock. 2021. Changes in the distribution of fitness effects and adaptive mutational spectra following a single first step towards adaptation. Nature Communications 12.

Blount, Z. D., C. Z. Borland, and R. E. Lenski. 2008. Historical contingency and the evolution of a key innovation in an experimental population of *Escherichia coli*. Proceedings of the National Academy of Sciences 105:7899–7906.

Blount, Z. D., R. E. Lenski, and J. B. Losos. 2018. Contingency and determinism in evolution: Replaying life's tape. Science 362.

Bonner, J. T. 1998. The origins of multicellularity. Integrative Biology: Issues, News, and Reviews 1:27–36.

———. 2009. The Social Amoebae: The Biology of Cellular Slime Molds. Princeton University Press, Princeton.

Boraas, M. E., D. B. Seale, and J. E. Boxhorn. 1998. Phagotrophy by flagellate selects for colonial prey: A possible origin of multicellularity. Evolutionary Ecology 12:153–164.

Brenner, S. 1974. The genetics of *Caenorhabditis elegans*. Genetics 77:71–94.

Bretscher, A. P., and D. Kaiser. 1978. Nutrition of *Myxococcus xanthus*, a Fuiting Myxobacterium. Journal of Bacteriology 133:763–768.

Brodie, E. D., and E. D. Brodie. 1999. Predator-Prey Arms Races. BioScience 49:557–568.

Bull, C. T., K. G. Shetty, and K. V. Subbarao. 2002. Interactions between myxobacteria, plant pathogenic fungi, and biocontrol agents. Plant Disease 86:889–896.

Claessen, D., D. E. Rozen, O. P. Kuipers, L. Søgaard-Andersen, and G. P. van Wezel. 2014. Bacterial solutions to multicellularity: a tale of biofilms, filaments and fruiting bodies. Nature Reviews Microbiology 12:115–124.

Cornforth, D. M., and K. R. Foster. 2015. Antibiotics and the art of bacterial war. Proceedings of the National Academy of Sciences of the United States of America 112:10827–10828.

Dahl, J. L., C. H. Ulrich, and T. L. Kroft. 2011. Role of phase variation in the resistance of *Myxococcus xanthus* fruiting bodies to *Caenorhabditis elegans* predation. Journal of Bacteriology 193:5081–5089.

DePas, W. H., A. K. Syed, M. Sifuentes, J. S. Lee, D. Warshaw, V. Saggar, G. Csankovszki, et al. 2014. Biofilm formation protects *Escherichia coli* against killing by *Caenorhabditis elegans* and *Myxococcus xanthus*. Applied and Environmental Microbiology 80:7079–7087.

Findlay, B. L. 2016. The Chemical Ecology of Predatory Soil Bacteria. ACS Chemical Biology 11:1502–1510.

Freund, L., M. La Fortezza, N. Mayrhofer, K. A. Schaal, and G. J. Velicer. 2024. MyxoEE: Myxobacteria Evolution Experiments.

Grosberg, R. K., and R. R. Strathmann. 2007. The Evolution of Multicellularity: A Minor Major Transition? Annual Review of Ecology, Evolution, and Systematics 38:621–654.

Herron, M., P. Conlin, and W. Ratcliff, eds. 2022. The Evolution of Multicellularity. Evolutionary Cell Biology (1st ed.). CRC Press, Boca Raton.

Herron, M. D. 2016. Origins of multicellular complexity: *Volvox* and the volvocine algae. Molecular Ecology 25:1213–1223.

Herron, M. D., J. M. Borin, J. C. Boswell, J. Walker, I.-C. K. Chen, C. A. Knox, M. Boyd, et al. 2019. De novo origins of multicellularity in response to predation. Scientific Reports 9:2328.

Hillesland, K. L., G. J. Velicer, and R. E. Lenski. 2009. Experimental evolution of a microbial predator's ability to find prey. Proceedings of the Royal Society B: Biological Sciences 276:459–67.

Holt, R. D. 1977. Predation, apparent competition, and the structure of prey communities. Theoretical Population Biology 12:197–229.

Holt, R. D., and M. B. Bonsall. 2017. Apparent Competition. Annual Review of Ecology, Evolution, and Systematics 48:447–471.

Holt, R. D., J. Grover, and D. Tilman. 1994. Simple Rules for Interspecific Dominance in Systems with Exploitative and Apparent Competition. The American Naturalist 144:741–771.

Hong, R. L., and R. J. Sommer. 2006. *Pristionchus pacificus*: A well-rounded nematode. BioEssays 28:651–659.

Kapsetaki, S. E., R. M. Fisher, and S. A. West. 2016. Predation and the formation of multicellular groups in algae. Evolutionary Ecology Research 17:651–669.

Kauffman, A., L. Parsons, G. Stein, A. Wills, R. Kaletsky, and C. Murphy. 2011. *C. elegans* positive butanone learning, short-term, and long-term associative memory assays. Journal of Visualized Experiments 1–10.

Kessin, R. H., G. G. Gundersen, V. Zaydfudim, M. Grimson, and R. L. Blanton. 1996. How cellular slime molds evade nematodes. Proceedings of the National Academy of Sciences of the United States of America 93:4857–4861.

Kreth, J., J. W. Lengeler, and K. Jahreis. 2013. Characterization of Pyruvate Uptake in Escherichia coli K-12. PLOS ONE 8.

Kroos, L., D. Wall, J. Muñoz-Dorado, P. I. Higgs, M. Singer, S. T. Islam, E. M. F. Mauriello, et al. 2025. Milestones in the development of *Myxococcus xanthus* as a model multicellular bacterium. Journal of Bacteriology (accepted).

La Fortezza, M., O. Rendueles, H. Keller, and G. J. Velicer. 2022*a*. Hidden paths to endless forms most wonderful: ecology latently shapes evolution of multicellular development in predatory bacteria. Communications Biology 5:977.

La Fortezza, M., K. A. Schaal, and G. J. Velicer. 2022*b*. Group Formation: On the Evolution of Aggregative Multicellularity. Pages 89–110 *in* M. D.

Herron, P. L. Conlin, and W. C. Ratcliff, eds. The Evolution of Multicellularity. CRC Press, Boca Raton.
La Fortezza, M., and G. J. Velicer. 2021. Social selection within aggregative multicellular development drives morphological evolution. Proceedings of the Royal Society B 288.
Livingstone, P. G., R. M. Morphew, and D. E. Whitworth. 2017. Myxobacteria are able to prey broadly upon clinically-relevant pathogens, exhibiting a prey range which cannot be explained by phylogeny. Frontiers in Microbiology 8:1–9.
Machado, F. A., A. Hubbe, D. Melo, A. Porto, and G. Marroig. 2019. Measuring the magnitude of morphological integration: The effect of differences in morphometric representations and the inclusion of size. Evolution 73:2518–2528.
Mayrhofer, N., G. J. Velicer, K. A. Schaal, and M. Vasse. 2021. Behavioral Interactions between Bacterivorous Nematodes and Predatory Bacteria in a Synthetic Community. Microorganisms 9:1362.
Melo, D., G. Garcia, A. Hubbe, A. P. Assis, and G. Marroig. 2016. EvolQG - An R package for evolutionary quantitative genetics [version 3; referees: 2 approved, 1 approved with reservations]. F1000Research 4.
Mendes-Soares, H., and G. J. Velicer. 2013. Decomposing Predation: Testing for Parameters that Correlate with Predatory Performance by a Social Bacterium. Microbial Ecology 65:415–23.
Morgan, A. D., R. C. MacLean, K. L. Hillesland, and G. J. Velicer. 2010. Comparative Analysis of *Myxococcus* Predation on Soil Bacteria. Applied and Environmental Microbiology 76:6920–6927.
Müller, S., S. N. Strack, S. E. Ryan, D. B. Kearns, and J. R. Kirby. 2015. Predation by *Myxococcus xanthus* induces *Bacillus subtilis* to form spore-filled megastructures. Applied and Environmental Microbiology 81:203–210.
Nair, R. R., M. Vasse, S. Wielgoss, L. Sun, Y.-T. N. Yu, and G. J. Velicer. 2019. Bacterial predator-prey coevolution accelerates genome evolution and selects on virulence-associated prey defences. Nature Communications 10:4301.
Nair, R. R., and G. J. Velicer. 2021. Predatory bacteria select for sustained prey diversity. Microorganisms 9:1–14.
Oksanen, J., F. G. Blanchet, M. Friendly, R. Kindt, P. Legendre, D. McGlinn, P. R. Minchin, et al. 2020. vegan: Community Ecology Package.
Pavlicev, M., J. M. Cheverud, and G. P. Wagner. 2009. Measuring Morphological Integration Using Eigenvalue Variance. Evolutionary Biology 36:157–170.
Pavlicev, M., and T. F. Hansen. 2011. Genotype-Phenotype Maps Maximizing Evolvability: Modularity Revisited. Evolutionary Biology 38:371–389.
Pentz, J. T., T. Limberg, N. Beermann, and W. C. Ratcliff. 2015. Predator Escape: An Ecologically Realistic Scenario for the Evolutionary Origins of Multicellularity. Evolution: Education and Outreach 8:13.
Pérez, J., J. Munoz-Dorado, A. F. Brana, L. J. Shimkets, L. Sevillano, and R. I. Santamaría. 2011. *Myxococcus xanthus* induces actinorhodin overproduction and aerial mycelium formation by *Streptomyces coelicolor*. Microbial Biotechnology 4:175–183.
Pires da Silva, A. 2013. *Pristionchus pacificus* protocols. WormBook 1–20.
R Core Team. 2024. R: A language and environment for statistical computing. R Foundation for Statistical Computing, Vienna, Austria.
Ratcliff, W. C., R. F. Denison, M. Borrello, and M. Travisano. 2012. Experimental evolution of multicellularity. Proceedings of the National Academy of Sciences 109:1595–1600.
Rendueles, O., and G. J. Velicer. 2017. Evolution by flight and fight: diverse mechanisms of adaptation by actively motile microbes. The ISME Journal 11:555–568.
Rendueles, O., P. C. Zee, I. Dinkelacker, M. Amherd, S. Wielgoss, and G. J. Velicer. 2015. Rapid and widespread de novo evolution of kin discrimination. Proceedings of the National Academy of Sciences 112:9076–9081.
RStudio Team. 2020. RStudio: Integrated Development for R. RStudio, PBC, Boston, MA.
Schaal, K. A., Y.-T. Nicco Yu, M. Vasse, and G. J. Velicer. 2022. Allopatric divergence of cooperators confers cheating resistance and limits the effects of a defector mutation. bioRxiv 2021.01.07.425765.
Schindelin, J., I. Arganda-Carreras, E. Frise, V. Kaynig, M. Longair, T. Pietzsch, S. Preibisch, S. Preibisch, et al. 2012. Fiji: An open-source platform for biological-image analysis. Nature Methods 9:676–682.
Shimkets, L. J., M. Dworkin, and H. Reichenbach. 2006*a*. The Myxobacteria. Pages 31–115 *in*The Prokaryotes. Springer New York, New York, NY.
Shimkets, L. J., M. Dworkin, and H. Reichenbach. 2006*b*. The Myxobacteria. Prokaryotes.
Stanley, S. M. 1973. An Ecological Theory for the Sudden Origin of Multicellular Life in the Late Precambrian. Proceedings of the National Academy of Sciences 70:1486–1489.
Stiernagle, T. 2006. Maintenance of *C. elegans*. Pages 1–11 *in*WormBook. The C. elegans Research Community, WormBook.
Velicer, G. J., L. Kroos, and R. E. Lenski. 1998. Loss of social behaviors by *Myxococcus xanthus* during evolution in an unstructured habitat. Proceedings of the National Academy of Sciences 95:12376–12380.
Velicer, G. J., L. Kroos, and R. E. Lenski. 2000. Developmental cheating in the social bacterium *Myxococcus xanthus*. Nature 404:598–601.
Velicer, G. J., G. Raddatz, H. Keller, S. Deiss, C. Lanz, I. Dinkelacker, and S. C. Schuster. 2006. Comprehensive mutation identification in an evolved bacterial cooperator and its cheating ancestor.

Proceedings of the National Academy of Sciences 103:8107–8112.
Velicer, G. J., and M. Vos. 2009. Sociobiology of the Myxobacteria. Annual Review of Microbiology 63:599–623.
Vos, M., and G. J. Velicer. 2009. Social Conflict in Centimeter-and Global-Scale Populations of the Bacterium *Myxococcus xanthus*. Current Biology 19:1763–1767.
Zee, P. C., H. Mendes-Soares, Y.-T. N. Yu, S. A. Kraemer, H. Keller, S. Ossowski, K. Schneeberger, et al. 2014. A shift from magnitude to sign epistasis during adaptive evolution of a bacterial social trait. Evolution 68:2701–2708.

Figures

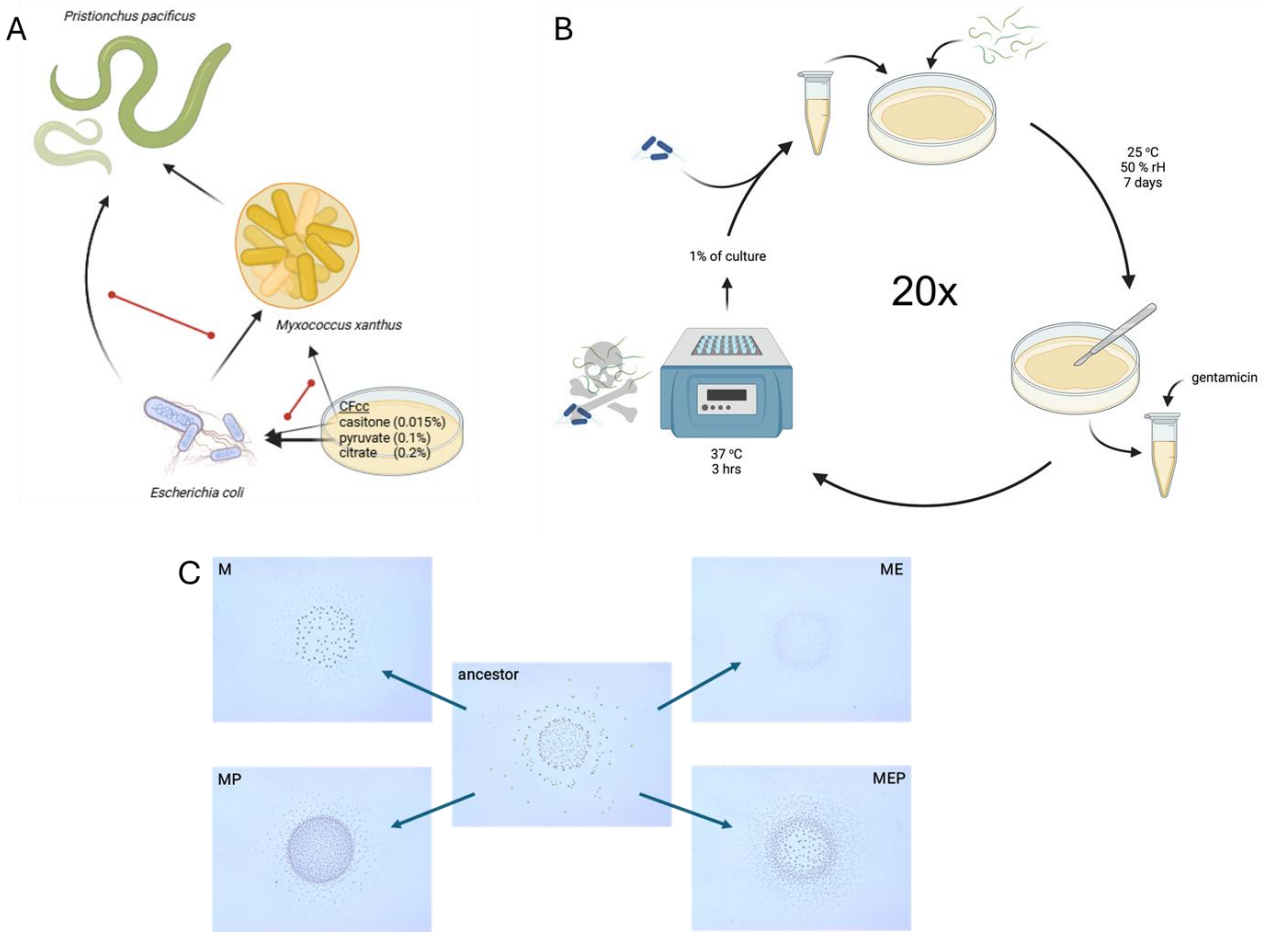

Figure 1. Experimental food web and evolution protocol. (A) We assembled a tri-trophic food web with *P. pacificus* as the apex predator, *M. xanthus* as the mesopredator, and *E. coli* as the basal prey. *E. coli* was sustained by carbon sources in the media, to which *M. xanthus* had partial access. Black arrows indicate energy flow (*e.g.,* via predation). Red double-headed lines indicate competition for resources. (B) Schematic showing the regime by which *M. xanthus* was transferred from cycle to cycle during the evolution experiment. (C) Images representing developmental diversification among evolved lineages. All images from the same ancestor. Created with BioRender.com.

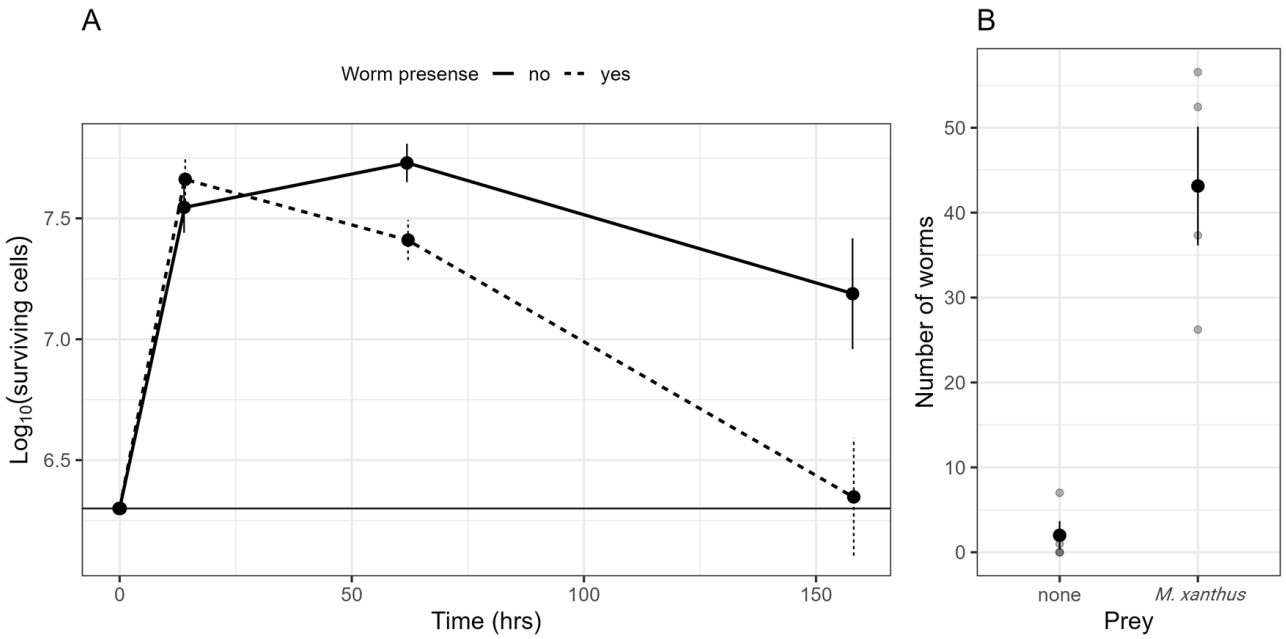

Figure 2. *Pristionchus pacificus* predation of *Myxococcus xanthus*. We cultured *P. pacificus* on *M. xanthus* as the sole food source. (A) Population dynamics of *M. xanthus* under predation by *P. pacificus*. The horizontal line shows the initial population size of *M. xanthus*. (B) *P. pacificus* reproduction on *M. xanthus*. Initial populations were founded with three J4 larvae. Large black dots are averages of four biological replicates. Small grey dots show individual replicates. *P. pacificus* population sizes after 72 hours are shown. Error bars represent standard error.

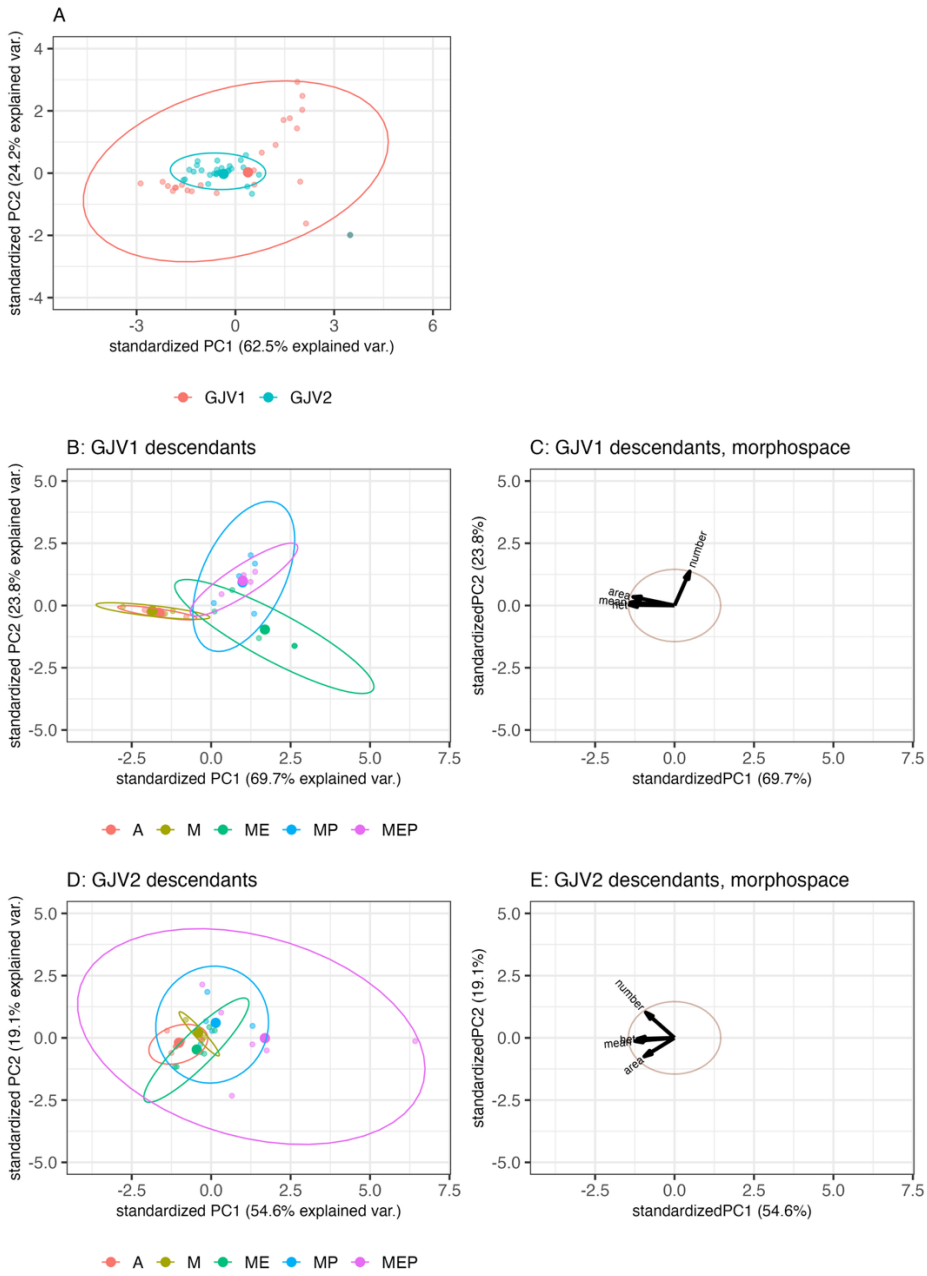

Figure 3. Evolutionary variation depends on ancestral genotype. We analyzed morphologies of fruiting bodies produced by *M. xanthus* populations that had evolved alone (M), in the presence of *E. coli* (ME), in the presence of *P. pacificus* (MP), or in the presence of both (MEP), as well as the clones used to found the evolved populations (A). Six of the founding clones come from GJV1 and six come from GJV2. We measured the principal components of variation across fruiting body traits. Here we show overall variation in fruiting body morphology as a function of the ultimate ancestor of the clones or evolved populations in the form of a principal components analysis of the four traits. Panel A shows the phenotypic variation within descendants of GJV1 versus descendants of GJV2. Panels B & D show trait variation based on evolution environment. Small dots represent averages across four replicates for each surviving lineage, large dots represent the centroid of each group (the average of PC1 and PC2 across all replicate lineages) and ellipses represent the 95% confidence region. Percentages listed in the x- and y-axis titles are the percent of variation within the dataset which is explained by that principal component. Panels C & E visualize the morphospaces, which consider how the four traits correlate, and which can be used to interpret the variation seen in panels B & D. Arrows indicate the directional effect of each trait on the morphospace – along that vector, the value of the indicated trait increases. Traits: “het” = fruiting body heterogeneity, “area” = fruiting body size, “mean” = fruiting body darkness, “number” = number of fruiting bodies produced by a defined population of cells.

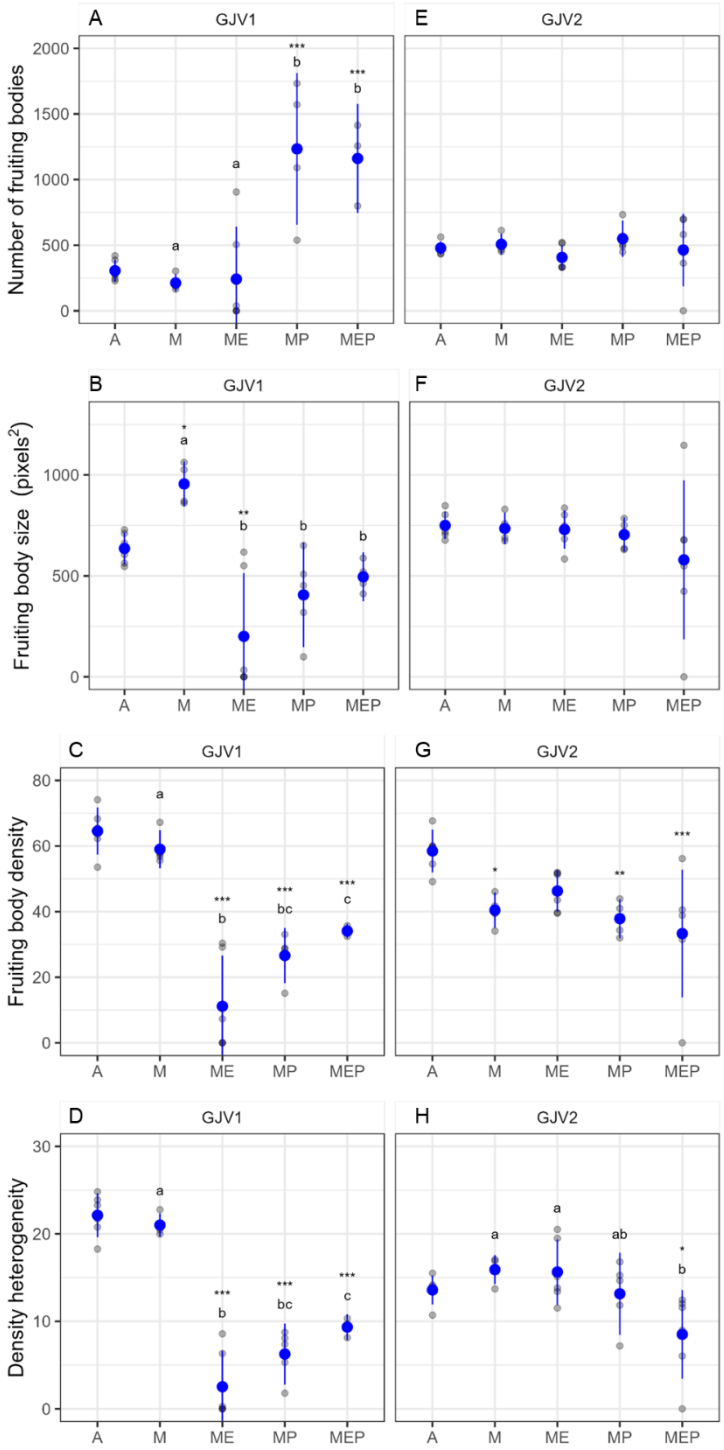

Figure 4. Fruiting body traits show evolutionary responses to community structure. Each measured trait of fruiting body morphology – number, size, density, and density heterogeneity – is plotted individually. We observe differences from the ancestral phenotype, represented by the founding clones (A on the x-axes) and differences among evolution treatments. Small grey dots show the mean of each evolution lineage across 3-4 biological replicates, large blue dots represent the mean across 4-6 replicate lineages, and blue bars show 95% confidence intervals of cross-lineage means. Asterisks indicate difference from the ancestors: * = $p < 0.05$, ** = $p < 0.01$, *** = $p < 0.005$. Letters indicate statistical groups of evolution treatments that do not differ within groups but differ between groups ($p < 0.05$). Vertical panels group clones or populations descending from GJV1 or from GJV2.

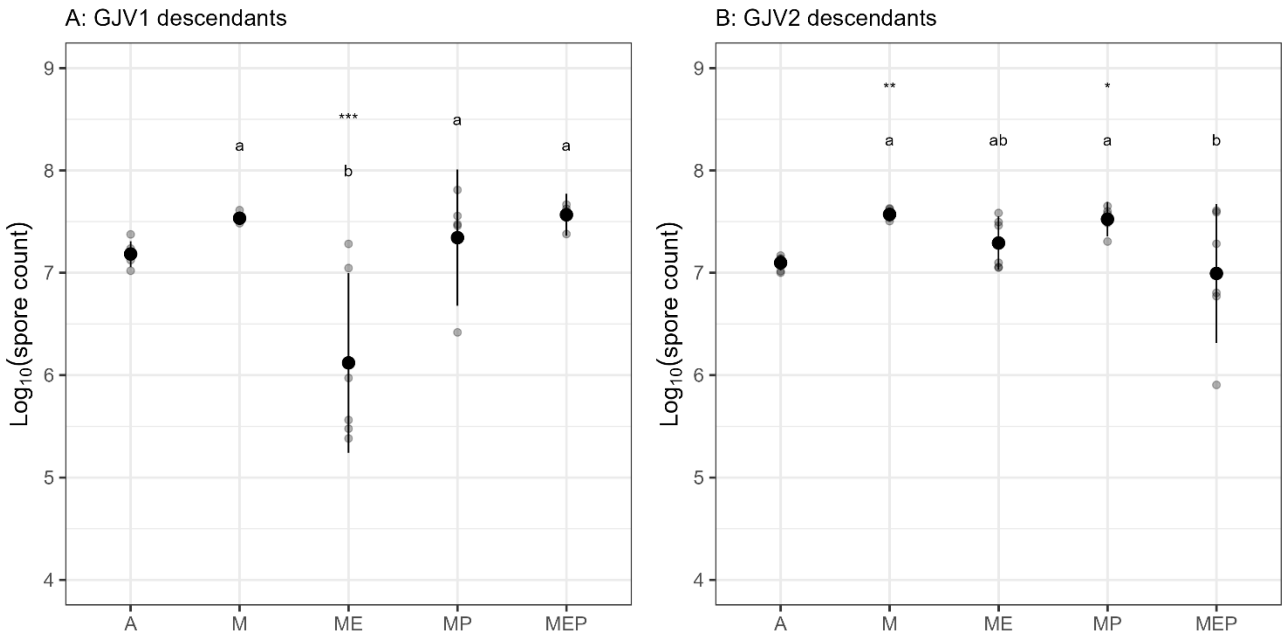

Figure 5. Spore production by GJV1 and GJV2 descendants. We counted the number of spores produced on each fruiting body morphology analysis plate. Small grey dots show the mean of each evolution lineage across 3-4 biological replicates, large black dots represent the mean across 4-6 replicate evolutionary lineages, and blue bars show 95% confidence intervals of cross-lineage means. Asterisks indicate difference from the ancestors: * = $p < 0.05$, ** = $p < 0.01$, *** = $p < 0.005$. Letters indicate statistical groups of evolution treatments that do not differ within groups but differ between groups ($p < 0.05$).

Supplemental information for:

Predation, evo-devo, and historical contingency: A nematode predator drives evolution of aggregative multicellularity

Kaitlin A. Schaal[1,2,*], Marco La Fortezza[2], & Gregory J. Velicer[2]

[1]Department of Evolution, Ecology & Behaviour, University of Liverpool, Liverpool, UK; [2]Institute of Integrative Biology, ETH Zürich, Zürich, Switzerland

* Corresponding author. Email: contact@kaitlinschaal.com

Contents:

Figure S1. Eigenvector analysis of pleiotropy among developmental traits.

Figure S2. Spore production by fruiting body number and size.

Table S1. Two-way ANOVA results for linear correlation between spore counts and fruiting body number or size.

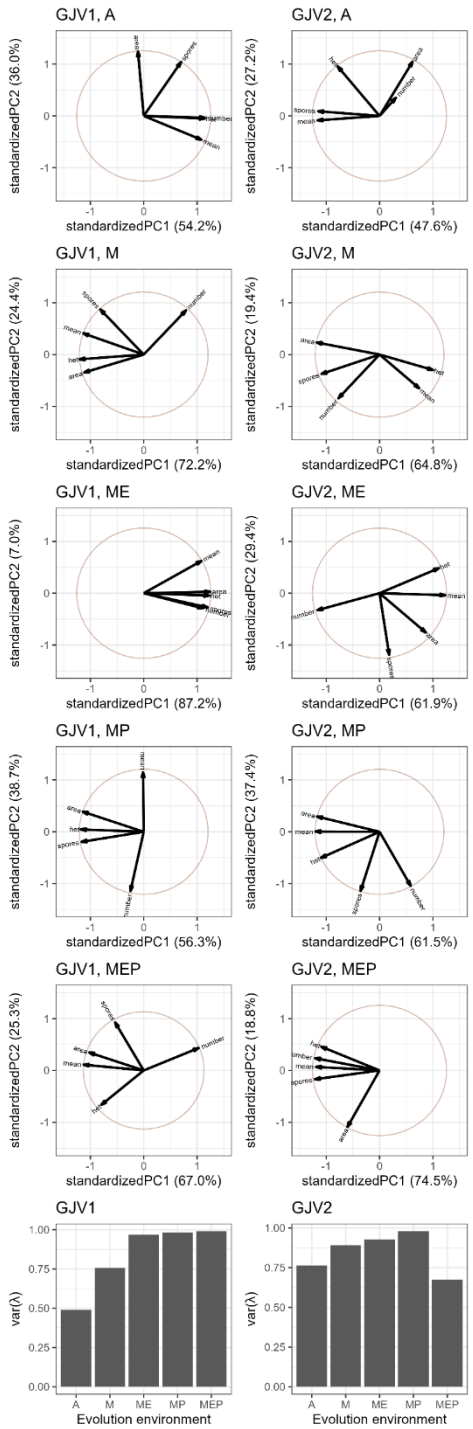

Figure S1. Eigenvector analysis of pleiotropy among developmental traits. Trait morphospaces of ancestral or evolved strains descending from GJV1 or GJV2, including fruiting body number, size, darkness, heterogeneity, and spore count; orthogonal arrows represent non-correlated traits. Bottom two panels show average eigenvector variance for the ancestral clones and each evolution environment. Traits: “het” = fruiting body heterogeneity, “area” = fruiting body size, “mean” = fruiting body darkness, “number” = number of fruiting bodies produced by a defined population of cells.

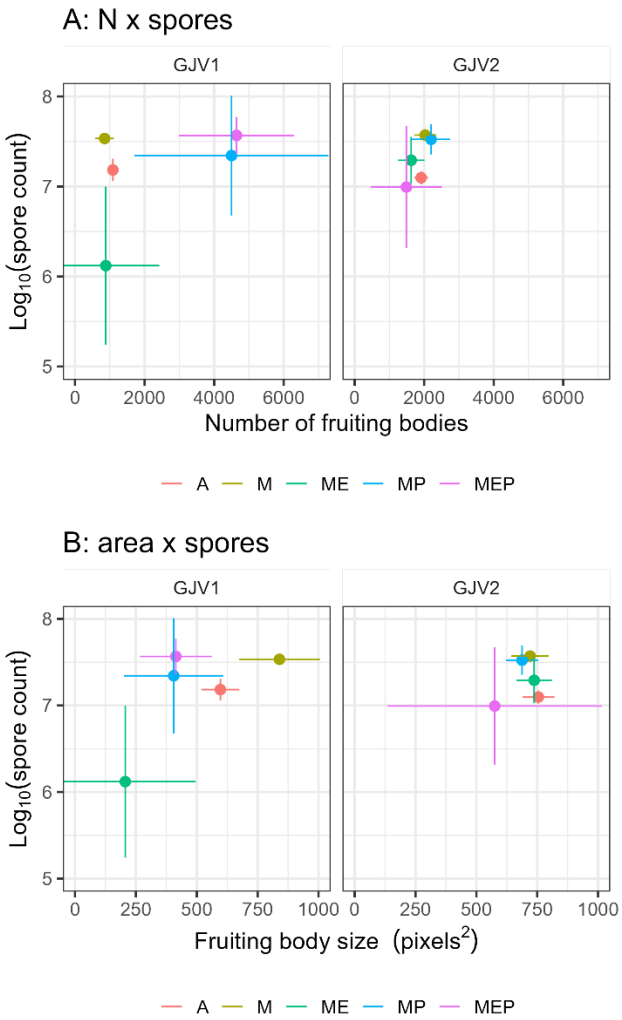

Figure S2. Spore production by fruiting body number and size. We show the relationship between spore production the number and size of fruiting bodies produced by descendants of GJV1 and GJV2. Dots represent the mean across 4-6 replicate lineages (each of which is calculated as a mean across 3-4 biological replicates), and bars show 95% confidence intervals of cross-lineage means. N = number of fruiting bodies, area = fruiting body size averaged within each plate, spores = number of spores produced. Spore counts are paired with the N or area value for the plate from which the spores were harvested. Panels group clones or populations descending from GJV1 or from GJV2.

Table S1. Two-way ANOVA results for linear correlation between spore counts and fruiting body number or size. df = degrees of freedom.

Source	df	*F*	*p*
N CFcc GJV1			
number	1	21.97	0.0002
treatment	4	11.11	0.0002
interaction	4	2.05	0.1356
residuals	16		
N CFcc GJV2			
number	1	64.87	< 0.0001
treatment	4	4.70	0.0090
interaction	4	2.52	0.0775
residuals	18		
area CFcc GJV1			
area	1	162.06	< 0.0001
treatment	4	21.51	< 0.0001
interaction	4	3.13	0.0442
residuals	16		
area CFcc GJV2			
area	1	9.06	0.0075
treatment	4	3.09	0.0424
interaction	4	0.19	0.9398
residuals	18		